2016

Effect of boron doping on nanostructure and magnetism of rapidly quenched Zr_2Co_{11}-based alloys

Yunlong Geng
University of Nebraska–Lincoln, gengyunlong@gmail.com

Wenyong Zhang
University of Nebraska-Lincoln, wenyong.zhang@unl.edu

Parashu Kharel
University of Nebraska-Lincoln, pkharel2@unl.edu

Shah R. Valloppilly
University of Nebraska-Lincoln, svalloppilly2@unl.edu

Ralph Skomski
University of Nebraska-Lincoln, rskomski2@unl.edu

See next page for additional authors

Effect of boron doping on nanostructure and magnetism of rapidly quenched Zr_2Co_{11}-based alloys

Yunlong Jin,[1,2] Wenyong Zhang,[1] Parashu R. Kharel,[1,3] Shah R. Valloppilly,[1] Ralph Skomski,[1] and David J. Sellmyer[1,2]
[1]*Nebraska Center for Materials and Nanoscience, University of Nebraska, Lincoln, NE 68588, USA*
[2]*Department of Physics and Astronomy, University of Nebraska, Lincoln, NE 68588, USA*
[3]*Department of Physics, South Dakota State University, Brookings, SD 57007, USA*

(Presented 15 January 2016; received 6 November 2015; accepted 19 November 2015; published online 18 February 2016)

The role of B on the microstructure and magnetism of $Zr_{16}Co_{82.5-x}Mo_{1.5}B_x$ ribbons prepared by arc melting and melt spinning is investigated. Microstructure analysis show that the ribbons consist of a hard-magnetic rhombohedral Zr_2Co_{11} phase and a minor amount of soft-magnetic Co. We show that the addition of B increases the amount of hard-magnetic phase, reduces the amount of soft-magnetic Co and coarsens the grain size from about 35 nm to 110 nm. There is a monotonic increase in the volume of the rhombohedral Zr_2Co_{11} unit cell with increasing B concentration. This is consistent with a previous theoretical prediction that B may occupy a special type of large interstitial sites, called interruption sites. The optimum magnetic properties, obtained for $x = 1$, are a saturation magnetization of 7.8 kG, a coercivity of 5.4 kOe, and a maximum energy product of 4.1 MGOe. [http://dx.doi.org/10.1063/1.4942556]

I. INTRODUCTION

Zr_2Co_{11}-based materials show promising intrinsic magnetic properties, including relatively high magnetocrystalline anisotropy, high Curie temperature, and hard magnetic properties, thus they have potential as cost-effective permanent magnets free of critical rare earths or expensive metals.[1–5] Alloys with the approximate stoichiometry Zr_2Co_{11} crystallize in cubic, orthorhombic, and rhombohedral structures, but only the rhombohedral phase, which is predicted to be metastable by formation-energy calculations, leads to significant coercivity.[3,5,6] The structures are basically dense-packed, with structural motifs reminiscent of that in $SmCo_5$.[6] Rhombohedral Zr_2Co_{11} is a high-temperature phase, whereas the orthorhombic phase is more stable at low temperatures. Rhombohedral Zr_2Co_{11} can therefore be produced by quenching the molten mixture so long as the quench rate is sufficiently high.[5,7–9] The higher the quench rate, the larger the content of rhombohedral Zr_2Co_{11} and the more refined the nanostructure, both enhancing the coercivity.[3,8]

However, binary Zr-Co ribbons have relatively low coercivities. There are several approaches to enhance coercivity in Zr_2Co_{11}. Metallic additives such as Ti, Si or Mo facilitate the formation of the hard-magnetic phase and decreases both the mean grain size and the amount of the soft Co phase.[5,10–12] The addition of Si and B has a similar effect.[3] In particular, boron addition has been found to increase the coercivity of rapidly quenched Zr-Co materials,[13,14] but it is unclear how B addition affects the phase components and structural properties. First-principle calculations[15] are consistent with both B substituting for Co and B occupying "interruption sites" between the motifs. The two occupancies can be distinguished experimentally by considering the unit-cell volume, which increases and decreases for interstitial and substitutional occupancies, respectively.

In this paper, we investigate how boron in melt-spun ribbons of $Zr_{16}Co_{82.5-x}Mo_{1.5}B_x$($x = 0,1,2,3,4$) affects the structural and magnetic properties. The main question is whether the B enters the rhombohedral Zr_2Co_{11} lattice interstitially or substitutionally.

II. EXPERIMENTAL METHODS

Ingots having the elemental compositions $Zr_{16}Co_{82.5-x}Mo_{1.5}B_x (x = 0,1,2,3,4)$ were prepared from high-purity elements by arc melting under argon atmosphere. The melt-spinning was conducted under argon atmosphere by ejecting the molten alloys from a quartz tube onto the surface of a copper wheel rotating at 30 m/s. This wheel speed was chosen, because it simultaneously maximizes the coercivity and the XRD peak intensity of the rhombohedral main phase for $x = 1$[3]. The ribbons are about 2 mm wide and 50 μm thick. The powder X-ray diffraction (XRD) patterns were collected using a PANalytical Empyrean X-ray diffractometer with Cu Kα radiation, and the nanostructure was investigated by a FEI Tecnai Osiris Transmission Electron Microscope (TEM). Room-temperature magnetization measurements were performed in a Quantum Design superconducting quantum interference device (SQUID) magnetometer in fields of up to 7 T. To determine saturation polarization and magnetocrystalline anisotropy constant, the law-of-approach-to-saturation method was used to fit the high-field part of the $M(H)$ curves. The phase components were examined by thermomagnetic measurements using a Quantum Design physical property measurement system (PPMS) at temperatures up to 900 K. The applied field was parallel to the length of the ribbons.

III. RESULTS AND DISCUSSION

The ribbons mainly contain a rhombohedral Zr_2Co_{11}-like phase and soft Co.[3,5] Figure 1(a) shows XRD patterns of nanocrystalline $Zr_{16}Co_{82.5-x}Mo_{1.5}B_x (x = 0,1,2,3,4)$ ribbons prepared at a wheel speed of 30 m/s. The diffraction-peak deconvolution was performed with a Gaussian function in Origin software. The relative intensity of the diffraction peaks from Co decreases with increasing x, indicating that B addition suppresses the segregation of Co. No diffraction peaks from Co or other phase were detected for x = 2, 3, 4, implying almost predominantly single phase Zr_2Co_{11}. The full-width at half-maximum (FWHM) of the Zr_2Co_{11} diffraction peaks at 44.45° decrease with increasing x, indicating that the mean grain size of rhombohedral Zr_2Co_{11} increases. By contrast, the FWHM of diffraction peaks from Co at 45.06° increase with increasing x, which suggests that the mean grain size of Co decreases. A widened peak around 45° was observed for $x \geq 4$, which means that excessive B addition leads to the formation of an amorphous phase resulting in the decrease of Zr_2Co_{11} phase content.

Figure 1(b) shows experimental and theoretical cell volumes of the Zr-Co phase as a function of the boron content. The theoretical values are from Ref. 15, where the boron content is calculated in atoms per unit cell (36 atoms). The experimental lattice parameters a, c and unit-cell volumes V of the rhombohedral Zr_2Co_{11} phase were determined by refining the XRD patterns using TOPAS (Total Pattern Analysis Solution) software. For $x = 0$, these values $a = 4.71$ Å, $c = 24.36$ Å, and $V = 469$ Å^3, for $x = 3$, they are $a = 4.74$ Å, $c = 24.45$ Å, and $V = 476$ Å^3. The slopes of the curves in Fig. 1(b) indicate that the B atoms enter the structure *interstitially*. The unit-cell volume

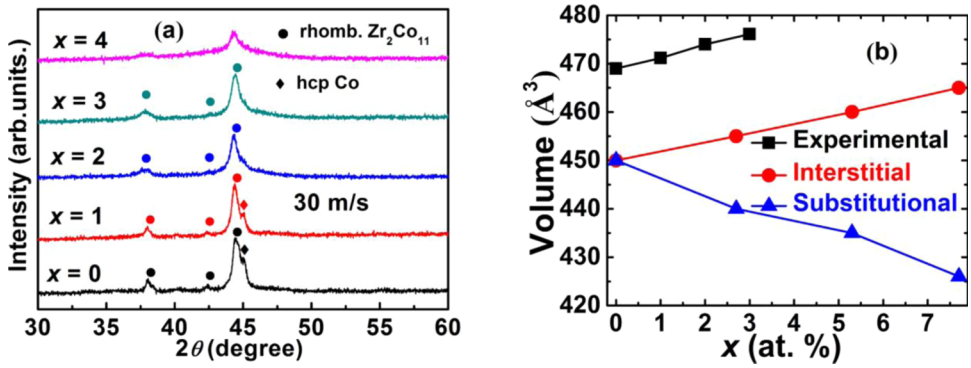

FIG. 1. Crystal structure of nanocrystalline $Zr_{16}Co_{82.5-x}Mo_{1.5}B_x$ ($x = 0$ - 4): (a) powder XRD patterns and (b) unit-cell volume as function of boron content. Interstitial and substitutional data from calculations of Ref. 15.

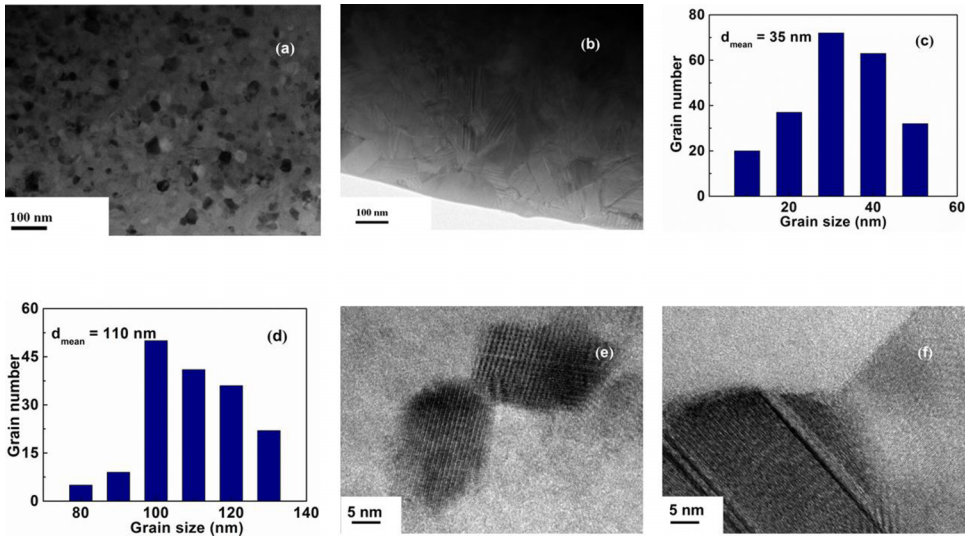

FIG. 2. TEM analysis of $Zr_{16}Co_{82.5-x}Mo_{1.5}B_x$: TEM images for (a) $x = 0$ and (b) $x = 1$, grain-size distribution for (c) $x = 0$, (d) $x = 1$, and high resolution TEM images for (e) $x = 0$, (f) $x = 1$.

expansion for $x = 3$ is about 1.5%, compared to about 1.2% predicted for interstitially occupied interruption sites.

The quantum-mechanical origin of the lattice expansion is the need which orthogonalize the wave functions of the interstitial and host electrons. For dense-packed metallic systems, this leads to prediction of an approximately constant lattice expansion per interstitial atom.[16,17] Rule-of-thumb values, extracted from various transition-metal rich-alloys ($R_2Fe_{17}N_x$, $R_2Fe_{17}C_x$, $R_2Fe_{17}Hx$, $R_2Fe_{14}B$) are 2 Å^3 for H, 8 Å^3 for B, and 6 Å^3 for C and N. The present value, about 6 Å^3 per B atom, is consistent with these estimates. Note that the volume expansion per interstitial atom is approximately independent of the steric or "hardcore" size of the interstice — very small interstices are energetically unfavorable, and the added atoms avoid interstitial occupancy.

Figure 2 shows TEM images of ribbons of $Zr_{16}Co_{82.5-x}Mo_{1.5}B_x$ ($x = 0, 1$) and the corresponding grain-size distributions. The grains in (a) are the rhombohedral Zr_2Co_{11} phase for $x = 0$ and have an average grain size of 35 nm (c). The relatively small grains in (a) are believed to be the soft-magnetic Co phase. The average grain size of the rhombohedral Zr_2Co_{11} increased from 35 nm for $x = 0$ to 110 nm for $x = 1$ (d), which is in good agreement with the XRD results of Fig. 1(a). The corresponding HRTEM images, Figs. 2(e)-2(f), show that the hard magnetic phase contains defects and twinned crystals, which contributes to the coercivity.

Figure 3(a) shows the temperature dependence of the magnetization for $x = 0$, 1, 3 in an applied field of 1 kOe. Figure 3(b) contains the corresponding derivatives dJ/dT from which the

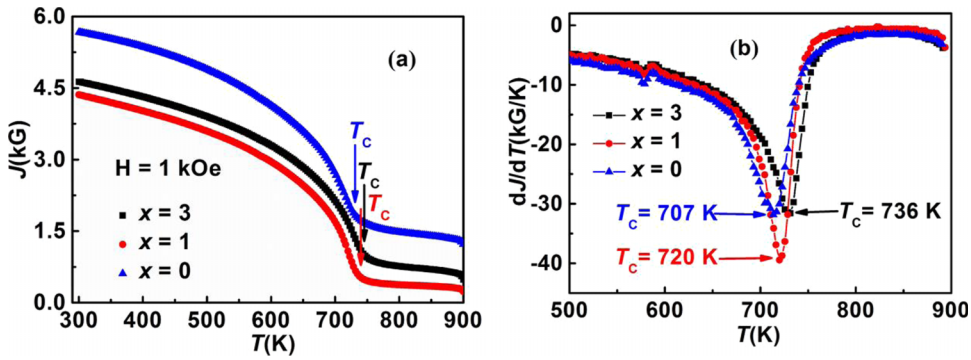

FIG. 3. Temperature dependence of the magnetization: (a) $J(T)$ and (b) dJ/dT.

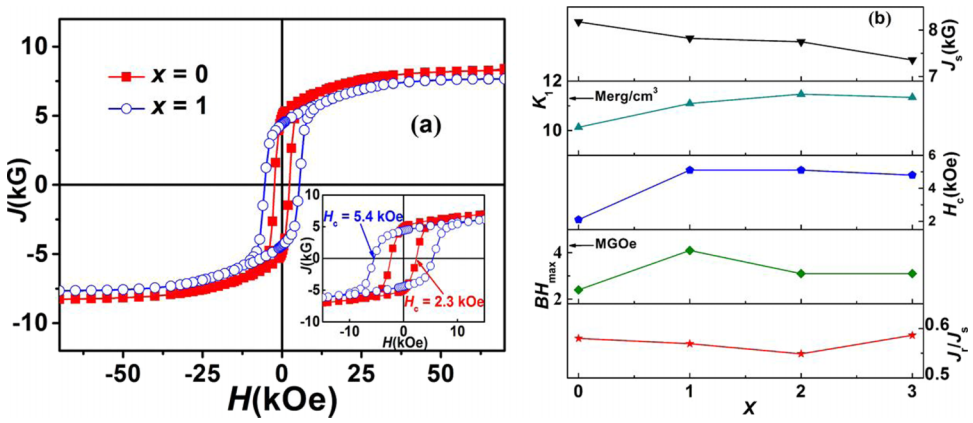

FIG. 4. Magnetic properties: (a) room-temperature hysteresis loops and (b) boron-content dependence of saturation polarization (J_s), anisotropy constant (K_1), intrinsic coercivity (H_c), maximum energy product ($(BH)_{max}$) and remanence ratio (J_r/J_s).

Curie temperatures of the rhombohedral phases were determined. A ferromagnetic-paramagnetic transition of the rhombohedral Zr_2Co_{11} phase is seen in all samples. The Curie temperatures increases from 707 K for $x = 0$ to 736 K for $x = 3$. This relatively small increase is consistent with Ref. 15 and probably reflects the effect of B on the electronic structure of the host. The amount of Co, estimated from Fig. 3(a), is 7.9 at% for $x = 0$ and 1.5 at% for $x = 1$. This means that B addition promotes the formation of the rhombohedral Zr_2Co_{11}-type phase.

Figure 4(a) shows the room temperature hysteresis loops for $x = 0$ and $x = 1$. The coercivity increases from 2.3 kOe for $x = 0$ to 5.4 kOe for $x = 1$, which is probably due to the increase in Zr_2Co_{11} phase. Simultaneously, the maximum energy product increases from 2.1 MGOe for $x = 0$ to 4.1 MGOe for $x = 1$. Figure 4(b) summarizes the B-content dependence of saturation polarization J_s, anisotropy constant K_1, coercivity H_c, maximum energy product $(BH)_{max}$ and remanence ratio J_r/J_s. J_s decreases with increase in x, mainly because the B suppresses the Co moment.[15] K_1 increases about 15% as the B content increases from $x = 0$ to $x = 3$, the change being comparable to the accuracy of the method. The absolute values are somewhat smaller than calculated in Ref. 15 (14 Merg/cm^3 for $x = 0$).

IV. CONCLUSIONS

The boron-content dependence of nanostructure and magnetic properties in melt-spun ribbons of nanocrystalline $Zr_{16}Co_{82.5-x}Mo_{1.5}B_x (x = 0, 1, 2, 3, 4)$ has been investigated. The main phase in ribbons is rhombohedral Zr_2Co_{11}. Addition of B gives rise to an expansion of the cell volume of the rhombohedral Zr_2Co_{11} phase, and the volume expansion of the lattice indicates interstitial B occupancy. Proper B addition enhances the content of hard magnetic phase and increases the average grain size, results in a coercivity increase by 91%. The best magnetic properties, namely $H_c = 5.4$ kOe, $(BH)_{max} = 4.1$ MGOe, and $J_s = 7.8$ kG, were obtained for the ribbon with $x = 1$. These properties are comparable to some grades of alnico and encourage further research on Zr-Co rare-earth-free permanent magnets.

ACKNOWLEDGMENT

This research was supported by NSF, DMR under Award DMREF: SusChEM 1436385. The work was performed in part in the Nebraska Nanoscale Facility, Nebraska Center for Materials and Nanoscience, which is supported by the National Science Foundation under Award ECCS: 1542182, and the Nebraska Research Initiative.

[1] E. Burzo, R. Grossinger, P. Hundegger, H. R. Kirchmayr, R. Krewenka, O. Mayerhofer, and R. Lemaire, "Magnetic-properties of $ZrCo_{5.1-x}Fe_x$ Alloys," J. Appl. Phys. **70**(10), 6550 (1991).
[2] G. V. Ivanova and N. N. Shchegoleva, "The Microstructure of a Magnetically Hard Zr_2Co_{11} Alloy," Phys. Met. Metall **107**(3), 270 (2009).
[3] W. Y. Zhang, S. R. Valloppilly, X. Z. Li, R. Skomski, J. E. Shield, and D. J. Sellmyer, "Coercivity Enhancement in Zr_2Co_{11}-Based Nanocrystalline Materials Due to Mo Addition," IEEE Trans. Magn **48**(11), 3603 (2012).
[4] B. Balasubramanian, B. Das, R. Skomski, W. Y. Zhang, and D. J. Sellmyer, "Novel Nanostructured Rare-Earth-Free Magnetic Materials with High Energy Products," Adv. Mater. **25**(42), 6090 (2013).
[5] Y. L. Jin, W. Y. Zhang, R. Skomski, S. Valloppilly, J. E. Shield, and D. J. Sellmyer, "Phase composition and nanostructure of Zr_2Co_{11}-based alloys," J. Appl. Phys. **115**(17), (2014).
[6] X. Zhao, M. C. Nguyen, W. Y. Zhang, C. Z. Wang, M. J. Kramer, D. J. Sellmyer, X. Z. Li, F. Zhang, L. Q. Ke, V. P. Antropov, and K. M. Ho, "Exploring the Structural Complexity of Intermetallic Compounds by an Adaptive Genetic Algorithm," Phys. Rev. Lett. **112**(4), (2014).
[7] B. G. Demczyk and S. F. Cheng, "Structure of Zr_2Co_{11} and $HfCo_7$ Intermetallic Compounds," J. Appl. Crystallogr. **24**, 1023-1026 (1991).
[8] A. M. Gabay, Y. Zhang, and G. C. Hadjipanayis, "Cobalt-rich Magnetic Phases in Zr-Co Alloys," J. Magn. Magn. Mater. **236**(1-2), 37 (2001).
[9] W. Y. Zhang, X. Z. Li, S. Valloppilly, R. Skomski, J. E. Shield, and D. J. Sellmyer, "Magnetism of Rapidly Quenched Rhombohedral Zr_2Co_{11}-based Nanocomposites," J. Phys. D: Appl. Phys. **46**(13), (2013).
[10] W. Y. Zhang, S. Valloppilly, X. Z. Li, Y. Liu, S. Michalski, T. A. George, R. Skomski, and D. J. Sellmyer, "Magnetic Hardening of Zr_2Co_{11}:(Ti, Si) Nanomaterials," J. Alloys Compd. **587**, 578 (2014).
[11] Z. Hou, W. Wang, S. Xu, J. Zhang, C. Wu, and F. Su, "Hard Magnetic Properties of Melt-Spun $Co_{82}Zr_{18-x}Ti_x$ Alloys," Physica B: Condens. Matter **407**(7), 1047-1050 (2012).
[12] H. W. Chang, C. F. Tsai, C. C. Hsieh, C. W. Shih, W. C. Chang, and C. C. Shaw, "Magnetic Properties Enhancement of Melt Spun CoZrB Ribbons by Elemental Substitutions," J. Magn. Magn. Mater. **346**, 74 (2013).
[13] T. Ishikawa and K. Ohmori, "Hard Magnetic Phase in Rapidly Quenched Zr-Co-B Alloys," IEEE Trans. Magn **26**(5), 1370-1372 (1990).
[14] T. Saito, "High Performance Co-Zr-B Melt-spun Ribbons," Appl. Phys. Lett. **82**(14), 2305-2307 (2003).
[15] X. Zhao, L. Ke, M. C. Nguyen, C.-Z. Wang, and K.-M. Ho, "Structures and Magnetic Properties of Co-Zr-B Magnets Studied by First-principles Calculations," J. Appl. Phys. **117**(24), 243902 (2015).
[16] J. D. Fast, *Gases in Metals* (Macmillan, London, 1976).
[17] R. Skomski, in *Rare-Earth—Iron Permanent Magnets*, edited by J. M. D. Coey (University Press, Oxford, 1996), pp. 178-217.